PCCP

RSC Publishing

PAPER

View Article Online
View Journal | View Issue

Cite this: *Phys. Chem. Chem. Phys.*, 2013, **15**, 19825

^{1}H-NMR measurements of proton mobility in nano-crystalline YSZ

Judith Hinterberg,*[a] Alina Adams,[b] Bernhard Blümich,[b] Paul Heitjans,[c] Sangtae Kim,[d] Zuhair A. Munir[d] and Manfred Martin*[a]

Received 30th July 2013,
Accepted 4th October 2013

DOI: 10.1039/c3cp53039f

www.rsc.org/pccp

We report nuclear magnetic resonance (NMR) results on water saturated, dense, nano-crystalline YSZ samples (9.5 mol% yttria doped zirconia) which exhibit proton conductivity at temperatures as low as room temperature. ^{1}H-NMR spectra recorded under static and magic angle spinning conditions show two distinct signals. Their temperature-dependent behavior and their linewidths suggest that one can be attributed to (free) water adsorbed on the surface of the sample and the other one to mobile protons within the sample. This interpretation is supported by comparison with measurements on a single-crystalline sample. For the nano-crystalline samples motional narrowing is observed for the signal originating from protons in the sample interior. For these protons, the analysis of temperature and field dependent spin-lattice relaxation time T_1 points towards diffusion in a confined two-dimensional geometry. We attribute this quasi two-dimensional motion to protons that are mobile along internal interfaces or nanopores of nano-crystalline YSZ.

1 Introduction

Yttria-stabilized cubic zirconia (YSZ) is well known for being an oxygen ion conductor at elevated temperatures, but its overall oxygen-ion conductivity decreases with a decrease in grain size, because space charge layers hinder the transport of oxygen ions across the grain boundaries.[1–4] Nano-structured cubic YSZ, however, shows an anomalously high conductivity at room temperature if exposed to a wet atmosphere. This has been attributed to proton conduction.[5] While this phenomenon only occurs in nano-crystalline samples, it is supposed that the enhanced conductivity is based on a grain-boundary mechanism,[6] or transport along internal interfaces and nanopores.[7]

We use ^{1}H-NMR to clarify the transport mechanism of protons incorporated into the dense, nano-crystalline samples. In a similar study Miyoshi *et al.* reported ^{1}H-NMR spectra of nano-crystalline tetragonal YSZ pellets.[8] They found interfacial hydrated layers between the nano-crystalline grains of the samples, as a result of the sample preparation. The reported spectra consist of three ^{1}H-NMR peaks which the authors assigned to surface-terminating hydroxyls, H_2O molecules that are H-bonded to these hydroxyls and free water molecules. These findings correspond well to the different layers of adsorbed water on cubic YSZ powders reported by Raz *et al.*[9] The samples investigated by Miyoshi *et al.* were compacted under ultra-high pressure and showed no macroscopic pores. The density of the samples was, however, significantly lower than the density of our pellets produced by Spark Plasma Sintering (SPS), which showed strong indications for room-temperature proton conductivity. In this paper we report results based on ^{1}H-NMR measurements on such hydrated, dense, nano-structured YSZ samples. With ^{1}H-NMR spectra under static and magic angle spinning (MAS) conditions we can directly probe the local environment and mobility of the protons incorporated into the samples instead of relying on indirect methods. In addition we measured the spin-lattice relaxation (SLR) times at different magnetic fields in a temperature range between room temperature and 110 °C. SLR provides a probe for self-diffusion, as the motion of the probed nuclei introduces temporal fluctuations to the local magnetic field (see, *e.g.*; ref. 10).

2 Experimental

2.1 Sample preparation

Nano-crystalline powders of 9.5 mol% YSZ were prepared by a precipitation method, employing nitrates ($Y(NO_3)_3{\cdot}6H_2O$, $ZrO(NO_3)_2{\cdot}6H_2O$, Aldrich, 99%) as precursors and aq. NH_4 as

[a] *Institute of Physical Chemistry, RWTH Aachen University, Germany. E-mail: martin@rwth-aachen.de*
[b] *Institute of Technical and Macromolecular Chemistry, RWTH Aachen University, Germany*
[c] *Institute of Physical Chemistry and Electrochemistry, Leibniz University Hannover, Germany*
[d] *Department of Chemical Engineering and Materials Science, University of California Davis, USA*

a precipitating agent. The obtained material was decanted and washed with water and ethanol. After drying at 100 °C for approximately 12 h, the material was ground in a mortar and pestle and then annealed in air at 450 °C for 2 h. The powder was subsequently consolidated to pellets by the Spark Plasma Sintering method.[11] The disc-shaped pellets obtained have a diameter of 5 mm and a thickness of 1 mm. The sintered samples have a relative density of 95.8% and higher, and grain sizes of *ca.* 30 nm, as determined from X-ray diffraction peak broadening.[12] Since the atmosphere in the SPS is reducing, the samples were reoxidized in dry air at 650 °C for 2 h. Finally the pellets were ground and polished with a 1 μm diamond-paste finish to achieve a surface roughness of approximately 50 nm. A commercially available 9.5 mol% YSZ single crystal (Crystec) sample was used for comparative measurements.

2.2 Water incorporation

The YSZ samples as such were saturated with water by storing them in distilled water at different temperatures (40–70 °C) for several days. The mass increase of the sample exposed to water at 70 °C for 47 h was determined by thermogravimetry (TG); the sample was heated to 700 °C in synthetic air and the mass loss was measured.

2.3 NMR measurements

Static ^{1}H-NMR spectra were recorded at different magnetic fields using the following spectrometers: a Bruker DSX 200 (B = 4.7 T), a Bruker MSL 400 (9.4 T), a Bruker DSX 500 (11.75 T) and a Bruker Ascend 600 (14.1 T). At 11.75 T, a 7 mm MAS probe and a zirconia rotor, at 4.7 T, a 10 mm probe and a glass tube, and at 9.4 T and 14.1 T, a 4 mm MAS probe and a zirconia rotor were used. The sample measured at 14.1 T had to be cut into half to fit into the 4 mm MAS rotor, later in the text named sample 1 (whole sample) and sample 1′ (half sample). The sample later in the text referred to as sample 2 is identical to sample 1 in chemical composition, density and average grain size. However, the samples are not necessarily identical with regard to their nanostructure. All static measurements were performed on the macroscopic pellets after drying the surfaces and rinsing them with acetone. To avoid any influences of the NMR probe, all measurements were repeated without YSZ samples, and any NMR signal originating from the probe was subtracted from the corresponding sample signal. The same procedure with background subtraction was used for the SLR and MAS measurements.

^{1}H-NMR-MAS spectra were collected at 9.4 T with a spinning rate of 10 kHz. To perform the MAS measurements, a water-saturated sample was ground, and the resulting powder was placed in the 4 mm zirconia rotor. ^{1}H spin-lattice relaxation of protons inside the nano-crystalline YSZ pellets was measured with the saturation recovery sequence at 14.1 T, 9.4 T and at 4.7 T. The temperature was varied from room temperature to 110 °C. To determine the spin-lattice relaxation time the spectra of every evolution time of the T_1 measurement were evaluated with pseudo-Voigt functions. The area of each peak was used for the relaxation curves, which could be described well in terms of a single exponential function.

3 Results and discussion

3.1 Water incorporation

Fig. 1 shows the TG-signal during heating of a water-saturated sample. To separate the influence of water adsorbed at the surface of the sample, the sample was held at room temperature for 7 h in a flow of synthetic air prior to the heating procedure (region I in Fig. 1). The observed subsequent mass loss of 70 μg during heating to 700 °C (region II in Fig. 1) corresponds to an average density of hydrogen atoms of $\approx$0.4 mol l^{-1}. This shows firstly that water was incorporated into the sample and secondly that the number of hydrogen atoms is sufficient for ^{1}H-NMR measurements. As expected, no mass increase is observed during the cooling process (region III in Fig. 1). Hence the mass loss in region II is not caused by a loss of oxygen from the polycrystalline sample.

3.2 ^{1}H NMR spectra

The static NMR spectrum of a nano-crystalline 9.5 mol% YSZ shows two distinct peaks that are independent of the applied magnetic field (Fig. 2): one peak at approximately 4.5 ppm (henceforth referred to as peak 1) and the other at approximately 1 ppm (peak 2), both relative to tetramethylsilane (TMS). At room temperature peak 1 has a linewidth of approximately 700 Hz while peak 2 has a broader linewidth of *ca.* 2500 Hz. The MAS spectrum (Fig. 2) also exhibits only two distinct peaks, confirming that no other peaks are hidden in the broader feature of peak 2 in the static spectrum. The intensity of peak 1 in the MAS spectrum is significantly higher than in the static measurements. The sample material had to be ground into powder to achieve a proper spinning frequency; hence the overall surface area was increased. As peak 1 can be attributed to water molecules on the sample surface (see the following paragraph) this may be an evidence for an equilibrium between the protons inside the sample and those on the surface. No significant proton signal was measured for dry samples.

Fig. 3 shows the spectra of a nano-crystalline sample (average grain size *ca.* 30 nm) and the corresponding 9.5 mol% YSZ single crystal. Both samples were exposed to water for 72 h at 70 °C.

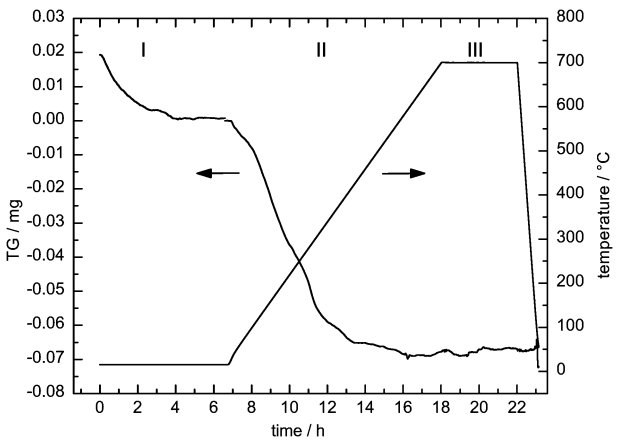

Fig. 1 A thermogravimetric measurement on a dense nano-crystalline YSZ sample hydrated in distilled water at 70 °C for 47 h.

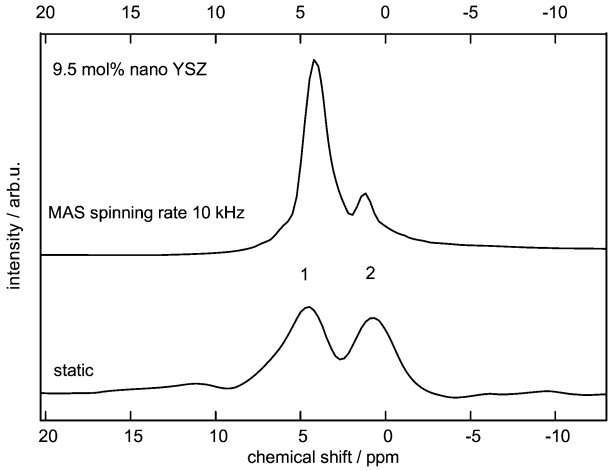

Fig. 2 Comparison of the MAS (upper graph) and the static (lower graph) ^{1}H-NMR spectra of 9.5 mol% nano-YSZ that was saturated with water at T = 50 °C. Both spectra were recorded at room temperature at 9.4 T. A spinning rate of 10 kHz was used to acquire the MAS spectrum.

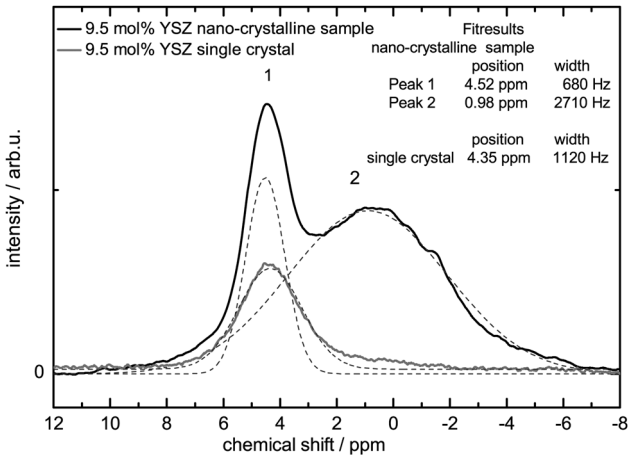

Fig. 3 Comparison between the static ^{1}H-NMR spectra of a 9.5 mol% nano-YSZ sample and the 9.5 mol% YSZ single crystal. Both samples were exposed to distilled water at 70 °C for three days and the corresponding spectra were recorded at 11.75 T at room temperature. The dashed lines are fits using pseudo-Voigt peak shapes to reproduce the spectra.

The spectrum of the single crystal shows only a single peak (chemical shift 4.5 ppm) at the same position as peak 1 in the spectrum of the nano-crystalline sample and with a similar linewidth but lower intensity than the latter. This peak position is close to the chemical shift of free water at 4.8 ppm.[13] As the same spectrum has been measured on a single crystal as well as a dry nano-crystalline sample only dipped into water, we attribute this peak to water adsorbed on the sample surface. The lower relative intensity of the peak observed for the single crystal compared to that of the nano-crystalline samples may be due to its relatively smaller effective surface as a result of a smaller surface roughness. Peak 2 that was found for the nano-crystalline samples is not present in the spectrum of the single-crystalline sample. As the solubility of water in YSZ single crystals is at least 40 times smaller than in nano-YSZ (which was shown by us using secondary ion mass spectrometry (SIMS) on D_2O saturated samples[14]) we can conclude that peak 2 is due to protons located in the "interior" of the nano-YSZ samples.

Temperature-dependent static NMR measurements between 32 and 62 °C (the measurements were performed in steps of 5 °C) show an increase of the intensity and a decrease of the linewidth of peak 2 with increasing temperature (Fig. 4a). This effect is reversible (Fig. 4b), and thus we attribute it to motional narrowing.[13] In contrast, peak 1 looses intensity and broadens with increasing temperature. This effect is irreversible, and therefore we attribute this behavior to the evaporation of a thin adsorbed water film on the surface of the macroscopic sample. This interpretation is consistent with the temperature dependent chemical shift of peak 1 which matches the behaviour observed for free water.[15]

The inset in Fig. 4a shows how the linewidth of peak 2 decreases as a function of increasing temperature. The linewidths were obtained by decomposition of the spectra with the help of two pseudo-Voigt functions. As peak 2 at low temperatures is only a weakly pronounced shoulder, the error of the

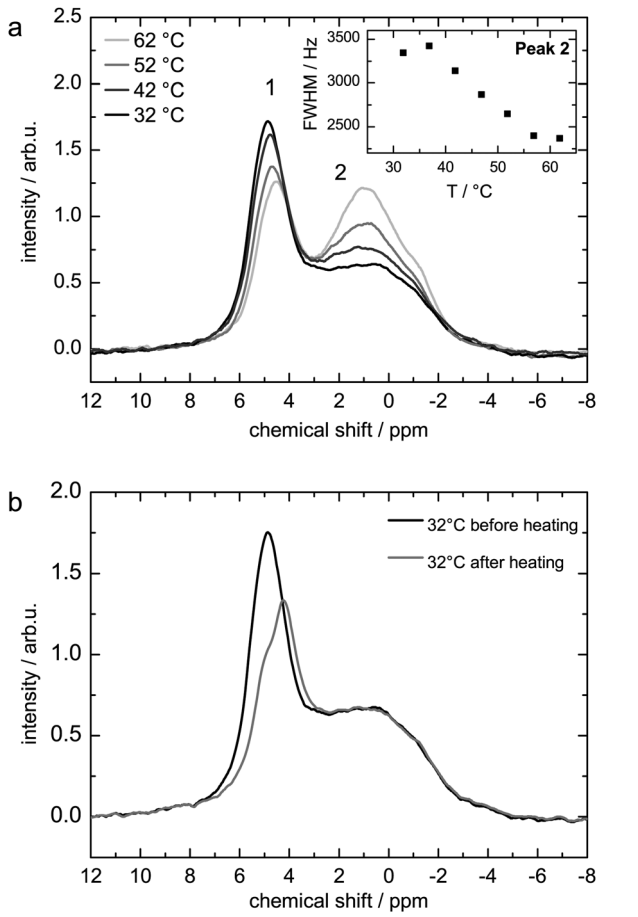

Fig. 4 (a) Static ^{1}H-NMR spectra of a dense, water saturated 9.5 mol% nano-YSZ sample at different temperatures. All spectra were recorded at 11.75 T. For the sake of clarity only four temperatures are shown in the graph. The inset shows the linewidth of peak 2. (b) The spectrum of the sample at 32 °C before and after heating.

linewidth is significant. For temperatures of 37 °C and higher, peak 2 was clearly visible and the linewidth decreases with increasing temperature. This finding indicates that the protons contributing to peak 2 belong in fact to mobile protons, in accordance with the reported proton conductivity in nano-cyrstalline YSZ.[5,6,14] Fig. 4b shows the spectra at 32 °C before and after the heating procedure. It is obvious that peak 2 returns to its original shape. But peak 1 shows a lower intensity, shifts to smaller chemical shifts and splits into two peaks, which may be an indicator for a higher amount of tightly bound water molecules on the sample surface after evaporation of the less tightly bound water molecules. All these findings support our interpretation that peak 1, at least partially, originates from a water film on the sample surface and that most of the water on the surface evaporates during heating.

In order to assign the two peaks observed in the ^{1}H NMR spectra we reviewed the literature. Chadwick *et al.* attributed a peak observed in the ^{1}H NMR spectrum of nano-crystalline zirconia located at 4.9 ppm to hydroxyl groups bounded to the sample surface, additional peaks observed at 2.7 ppm, 0.7 ppm and 0 ppm were ascribed to organic remains from the sol–gel preparation, as they disappeared after heat treatment.[16] Miyoshi *et al.* found three peaks in the ^{1}H-NMR spectrum of nano-crystalline tetragonal YSZ and assigned the peak located at 1.1 ppm to surface-terminating hydroxyls, the peak at 3.6 ppm to water molecules H-bonded to these hydroxyls and the peak at 5.4 ppm to free water molecules.[8] Similar ^{1}H NMR spectra were reported for mesoporous silica (SBA-15): a peak reported at approx. 1.7 ppm was assigned to hydroxyl groups bonded to the silicon atoms, and broader features measured at approx. 3 pmm and 5 ppm to weakly bonded water molecules and free water, respectively.[17,18] In the case of nano-crystalline anatase surface-terminating OH-groups were reported at 3.7 ppm, intermediately bonded water molecules at 5.5 ppm and free water molecules at 4 ppm.[19] Except for the case of nano-crystalline zirconia the ^{1}H NMR studies on nano-crystalline or mesoporous oxides found three contributions to the NMR spectrum, while we observe only two peaks even under MAS conditions and high temperatures. The chemical shift of peak 2 suggests an assignment to hydroxls in comparison to the abovementioned studies. This peak is only observed in the nano-crystalline samples, which have a high relative density, the assignment to hydroxyls seems therefore natural. But IR-measurements on comparable samples did not show any indications for OH-groups.[7] Peak 1, which we attribute to water molecules adsorbed on the sample surface, shows a splitting in two peaks after heating, thus leading to the conclusion that peak 1 could indeed consist of two peaks: one of water molecules or hydroxyl strongly bonded to the surface with a smaller chemical shift of approx. 3.5 ppm and one for weakly bonded, *i.e.* free water molecules at the chemical shift of approx. 4.7 ppm. Furthermore, if we adopt the assignment made by Miyoshi *et al.*, one cannot rule out that free water molecules or H-bonded water molecules from the sample interior contribute to the intensity of peak 1. At this point we cannot finalize the assignment of the proton signals. However the overall conclusion remains unaffected: as peak 2 is only found in the ^{1}H-NMR spectra of the nano-crystalline samples and shows motional narrowing these protons are most likely the origin of the reported low-temperature proton conduction in nano-crystalline YSZ.

3.3 Spin-lattice relaxation

The spin-lattice relaxation time T_1 is the (temperature- and field dependent) time constant describing the rate of recovery of the longitudinal component of the magnetization vector towards the thermodynamic equilibrium.[15] The underlying dynamic process relevant here is the diffusion of protons. For three-dimensional translational diffusion, ${T_1}^{-1}$ is given by the well-known expression developed by Bloembergen, Purcell and Pound (BPP):[15,20]

$$ {T_1}^{-1} = C \cdot \left[\frac{\tau_C}{1+\omega^2{\tau_C}^2} + \frac{4\tau_C}{1+4\omega^2{\tau_C}^2} \right] \quad (1) $$

where ω is the Larmor frequency of the NMR experiment and C is a constant. The correlation rate ${\tau_C}^{-1}$, which is directly related to the temperature dependent jump rate τ^{-1} of the atomic diffusion process, is given by:

$$ {\tau_C}^{-1} = {\tau_0}^{-1} \cdot \exp\left(-\frac{E_A}{RT}\right) \quad (2) $$

Here τ_0 is the pre-exponential factor, E_A is the activation energy, R is the gas constant, and T is the absolute temperature.

Based on the BPP-model the plot of $\log {T_1}^{-1}$ *versus* reciprocal temperature exhibits three typical features:

(i) ${T_1}^{-1}$ shows a maximum when the correlation rate ${\tau_C}^{-1}$ is approximately equal to the Larmor frequency ω. The position of the maximum shifts to higher temperatures with increasing frequency ω.

(ii) The plot is symmetrical, as the slopes of the low-temperature flank ($\omega\tau_C \gg 1$) with ${T_1}^{-1} \propto {\tau_C}^{-1}$ and the high-temperature flank ($\omega\tau_C \ll 1$) with ${T_1}^{-1} \propto \tau_C$ differ only in sign $-E_A/R$ and E_A/R, respectively.

(iii) In the high-temperature regime, there is no field dependence of the spin-lattice relaxation rate.

The spin-lattice relaxation rate ${T_1}^{-1}$ corresponding to peak 2 of two nano-crystalline YSZ samples was measured at different magnetic fields (4.7 T for sample 1, 14.1 T for sample 1′, and 9.4 T for sample 2) at various temperatures between room temperature and 110 °C (Fig. 5). In all cases the spectra belonging to the various evolution times of the T_1 measurement were reproduced by two pseudo-Voigt peaks referring to peak 1 and peak 2 and the corresponding peak area was used for the relaxation curves, which could be analyzed by a single exponential function. Through this approach we ensure that the signal of peak 1 does not interfere in the T_1 measurement of peak 2. The results show that the features (ii) and (iii) of BPP behavior are not fulfilled. The absolute values of the slopes of the high- and low-temperature flanks are not identical. This failure of the BPP model is demonstrated by the dashed lines in Fig. 5 which refer to an attempt to fit the experimental data points with eqn (1). For sample 1 a field dependence is found (squares in Fig. 5): both high-temperature flanks show different,

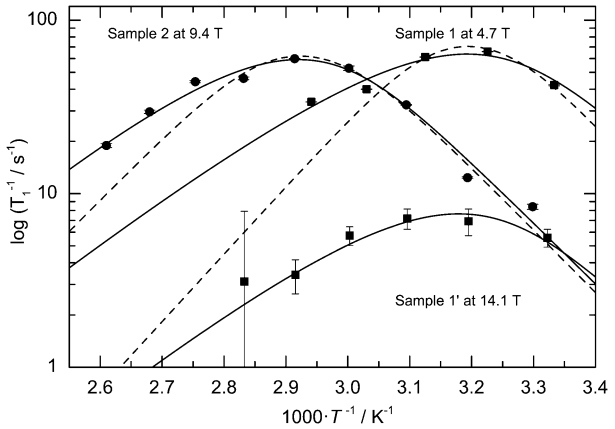

Fig. 5 Temperature dependence of the ^{1}H spin-lattice relaxation rate of two water saturated 9.5 mol% nano-YSZ samples (shown as squares for sample 1 and circles for sample 2) at three different magnetic fields (4.7 T, 9.4 T and 14.1 T). The dashed lines refer to BPP-model fits according to eqn (1), while the solid lines show fits according to the Richards expression (eqn (3)) for 2D diffusion.

i.e. field dependent, slopes and with increasing magnetic field the maximum is slightly shifted to higher temperatures. For sample 2 (circles in Fig. 5) the maximum is strongly shifted to higher temperatures compared to sample 1, which cannot be explained by the frequency dependence of the maximum. This shows that the relaxation behavior varies for different samples. The only difference between the samples, however, lies within the nano-structure, *i.e.* the amount and size of nano-pores. The phenomenon responsible for peak 2 is therefore probably not a material characteristic phenomenon like transport in the grain boundaries but more likely caused by different nano-structures of the samples, *i.e.* different internal surfaces and/or nano-pores, which can significantly vary from sample to sample and even in different areas of one sample. However, sample 2 also shows that low- and high-temperature flanks exhibit different slopes.

Other deviations from the symmetric BPP behavior can occur if one assumes a Gaussian distribution of activation energies for example in slightly disordered systems. Measuring spin-lattice relaxation in water saturated Y-doped $SrCeO_3$, Maekawa *et al.* observed an asymmetric temperature dependence of the spin-lattice relaxation rates.[21] They achieved a good fit using the BPP model with a Gaussian distribution of activation energies, the centre being set to 66 kJ mol^{-1} to coincide with conductivity data. But this should neither affect the high-temperature flank nor would a field dependence occur,[22] thus, these effects cannot explain the behaviour shown in Fig. 5.

Guided by our previous experimental findings indicating that protons are mobile only along internal interfaces of nano-YSZ (corresponding to quasi two-dimensional diffusion)[6,7,14] we use an empirical model developed by Richards to analyse our experimental data.[23] It considers two-dimensional motion and approximates the spin-lattice relaxation rate by:

$$T_1^{-1} = C \cdot \tau_C \cdot \ln\left(1 + \frac{1}{(\omega\tau_C)^2}\right) \qquad (3)$$

Table 1 Fit parameters of the 2D-model fit according to eqn (3) of the experimental data in Fig. 5

Field strength/T	Sample 1 4.7	Sample 1′ 14.1	Sample 2 9.4
$C \times 10^{10}$/S^{-2}	4.7 ± 1.7	0.6 ± 0.1	4.3 ± 0.6
$\log \tau_0$/s	−19.05 ± 1	−18.54 ± 1	−18.64 ± 1
E_A/kJ mol^{-1}	60 ± 30	63 ± 19	63 ± 13

The parameters C, τ_C and ω have a meaning analogous to that in eqn (1). The expression has been successfully used for well known 2D systems.[24–27]

While fitting the data sets obtained at field strengths of 14.1 T, 9.4 T and 4.7 T independently (solid curves in Fig. 5) the fit parameters C, τ_0 and E_A are in good agreement (see Table 1). The strong frequency dependence observed in the SLR of sample 1 however, is far bigger than predicted for 2D diffusion. Sample 1 had to be cut into halfs to fit into the 4 mm MAS rotor for the measurements at 14.1 T. This explains the deviation from the 2D model, as the signal of peak 2 orginates from protons within the nanoporous interior of the sample.[7] However, the difference in the slopes of the high- and low-temperature flank and the good agreement of the fit results remain as indications for two-dimensional motion of the incorporated protons, which would be expected for proton conduction in surface-terminating hydroxyls or H-bonded water molecules on them.

The obtained activation energies for the motion of protons in nanocrystalline YSZ are comparable to values found in Nafion by Slade *et al.* also using NMR relaxation experiments.[28] Slade *et al.* measured the spin-lattice relaxation rate with the inversion recovery sequence and fitted the temperature dependent results with a BPP-based model using a Gaussian distribution of activation energies. They obtained mean activation energies between 43.4 and 60.7 kJ mol^{-1}. Their pre-exponential factor τ_0 ranges from 10^{-23} to 10^{-18} s. Their values – as well as ours – are by far too small for an atomic hopping process. But Slade *et al.* claim that such a behavior "is typical of liquid-like behavior of adsorbed water and related systems".[28] However, our temperature range is by far too small to draw any further conclusion, but our values of τ_0 show the good agreement of our independent fits.

4 Conclusion

We investigated proton transport in a water saturated nanocrystalline 9.5 mol% YSZ sample using NMR measurements. ^{1}H-NMR spectra – under static as well as MAS conditions – only show two distinct signals. We attribute peak 1 at approximately 4.5 ppm to a thin water film on the sample surface and peak 2 at *ca.* 1 ppm to protons within the sample, which are not located within the nano-crystalline grains. The temperature-dependent behavior of the linewidth, intensity and spin-lattice relaxation time of peak 2 suggest that this peak originates from mobile protons or protonic defects, moving in a two-dimensional environment in the nano-crystalline YSZ. Since the corresponding single crystal shows no evidence for protons in the interior of

the material we conclude that the internal surfaces are the only possible pathway for protons in the sample, in agreement with impedance data[6] and IR measurements.[7]

Acknowledgements

We would like to thank Martin Wilkening and Viktor Epp for the fruitful discussions and support with the NMR measurements.

References

1 M. Verkerk, B. Middlehuis and A. Burggraaf, *Solid State Ionics*, 1982, **6**, 159–170.
2 X. Guo and R. Waser, *Prog. Mater. Sci.*, 2006, **51**, 151–210.
3 N. Perry, S. Kim and T. Mason, *J. Mater. Sci.*, 2008, **43**, 4684–4692.
4 R. A. De Souza, M. J. Pietrowski, U. Anselmi-Tamburini, S. Kim, Z. A. Munir and M. Martin, *Phys. Chem. Chem. Phys.*, 2008, **10**, 2067.
5 S. Kim, U. Anselmi-Tamburini, H. J. Park, M. Martin and Z. A. Munir, *Adv. Mater.*, 2008, **20**, 556–559.
6 S. Kim, H. J. Avila-Paredes, S. Wang, C.-T. Chen, R. A. De Souza, M. Martin and Z. A. Munir, *Phys. Chem. Chem. Phys.*, 2009, **11**, 3035.
7 M. Pietrowski, R. De Souza, A. Reinholdt, Z. A. Munir, M. Martin and S. Kim, *Solid State Ionics*, 2012, **225**, 241–244.
8 S. Miyoshi, Y. Akao, N. Kuwata, J. Kawamura, Y. Oyama, T. Yagi and S. Yamaguchi, *Solid State Ionics*, 2012, **207**, 21–28.
9 S. Raz, K. Sasaki, J. Maier and I. Riess, *Solid State Ionics*, 2001, **143**, 181–204.
10 P. Heitjans, A. Schirmer and S. Indris, in *Diffusion in condensed Matter*, ed. P. Heitjans and J. Kärger, Springer, Berlin and Heidelberg, 2005, pp. 367–413.
11 D. V. Quach, H. Avila-Paredes, S. Kim, M. Martin and Z. A. Munir, *Acta Mater.*, 2010, **58**, 5022–5030.
12 D. Quach, S. Kim, R. De Souza, M. Martin and Z. Munir, *Key Eng. Mater.*, 2011, **484**, 107–116.
13 H. E. Gottlieb, V. Kotlyar and A. Nudelman, *J. Org. Chem.*, 1997, **62**, 7512–7515.
14 H. J. Avila-Paredes, E. Barrera-Calva, H. U. Anderson, R. A. De Souza, M. Martin, Z. A. Munir and S. Kim, *J. Mater. Chem.*, 2010, **20**, 6235.
15 A. Abragam, *The Principles of Nuclear Magnetic Resonance*, Clarendon Press, Oxford University Press, Oxford, 1961.
16 A. Chadwick, G. Mountjoy, V. Nield, J. Poplett, M. Smith, J. Strange and M. Tucker, *Chem. Mater.*, 2001, **13**, 1219–1229.
17 J. Hu, J. Kwak, J. Herrera, Y. Wang and C. Peden, *Solid State Nucl. Magn. Reson.*, 2005, **27**, 200–205.
18 B. Grünberg, T. Emmler, E. Gedat, I. Shenderovich, G. Findenegg, H.-H. Limbach and G. Buntkowsky, *Chem.–Eur. J.*, 2004, **10**, 5689–5696.
19 J. Soria, J. Sanz, I. Sobrados, J. Coronado, A. Maira, M. Herández-Alonso and F. Fresno, *J. Phys. Chem. C*, 2007, **111**, 10590–10596.
20 N. Bloembergen, E. Purcell and R. Pound, *Phys. Rev.*, 1948, **73**, 679–712.
21 H. Maekawa, N. Kashii, J. Kawamura, Y. Hinatsu and T. Yamamura, *Solid State Ionics*, 1999, **122**, 231–236.
22 I. Svare, F. Borsa, D. Torgeson and S. Martin, *Phys. Rev. B: Condens. Matter Mater. Phys.*, 1993, **48**, 9336–9344.
23 P. Richards, in *Topics in Current Physics*, ed. M. Salamon, Springer, Berlin, 1979, ch. 6, vol. 15.
24 W. Küchler, P. Heitjans, A. Payer and R. Schöllhorn, *Solid State Ionics*, 1994, **70/71**, 434–438.
25 H. Ebinger, H. Jänsch, C. Polenz, B. Polivka, W. Preyss, V. Saier, R. Veith and D. Fick, *Phys. Rev. Lett.*, 1996, **76**, 656–659.
26 D. H. MacDonald, C. A. Sholl and P. C. L. Stephenson, *J. Phys.: Condens. Matter*, 1998, **10**, 417–428.
27 M. Wilkening, W. Küchler and P. Heitjans, *Phys. Rev. Lett.*, 2006, **97**, 065901.
28 R. Slade, A. Hardwick and P. Dickens, *Solid State Ionics*, 1983, **9, 10**, 1093–1098.

